

## Non-Destructive Inspection of Surface Integrity in Milled Turbine Blades of Inconel 738LC

KOLAŘÍK Kamil<sup>1, a</sup>, PALA Zdenek<sup>2, b</sup>, ČAPEK Jiří<sup>3, c</sup>, BERÁNEK Libor<sup>4, d</sup>  
VYSKOČIL Zdeněk<sup>5, e</sup> and GANEV Nikolaj<sup>6, f</sup>

<sup>1, 2, 3, 6</sup>Department of Solid State Engineering, Faculty of Nuclear Sciences and Physical Engineering, CTU in Prague; Trojanova 13, 120 00 Prague 2, Czech Republic

<sup>4</sup>Department of Manufacturing Technology, Faculty of Mechanical Engineering, CTU in Prague, Technická 4, 166 07 Prague 6, Czech Republic

<sup>5</sup>Industry Division, PBS Velká Bíteš, a. s., Vlkovská 279, 595 12 Velká Bíteš, Czech Republic

<sup>a</sup>kamil.kolarik@email.cz, <sup>b</sup>zdenek.pala@jfifi.cvut.cz, <sup>c</sup>ge.capek@seznam.cz,

<sup>d</sup>libor.beranek@fs.cvut.cz, <sup>e</sup>vyskocil.z@pbsvb.cz and <sup>f</sup>nikolaj.ganev@jfifi.cvut.cz

**Keywords:** Residual stresses, milling, geometrical product specification, nickel super-alloys, turbine blades.

**Abstract.** Nickel super-alloys are widely used in aerospace as material for turbine blades. Unfortunately, their machining is difficult since mechanical hardening and, consequently, extreme tool wear occur. Casting can no longer meet the requirements for precision, hence, the castings are being ground or milled. In this contribution, a quality check of the milled surface by several surface integrity parameters is proposed with respect to the surface structural inhomogeneities caused by mutual effect of plastic deformations and thermal fields during the cutting process. Castings from Inconel 738LC were milled with cutting conditions chosen by Design-Of-Experiments method and the resulting surfaces were assessed by non-destructive X-ray diffraction methods in several areas corresponding to various cutter orientation and work-piece angle. Surface integrity was described by macroscopic residual stresses, microstrains, grain sizes and phase composition. Mostly, favourable compressive surface residual stresses were observed in the cutting direction, grain sizes were distinctively smaller when the tool axis was perpendicular to the machined surface.

### 1. Introduction

Cooperation between industry and research institutes can often broaden the production lines and even help to find new markets. This is exactly the case of the present contribution which is aimed at extension of the technological possibilities enabling to machine castings from nickel super-alloy. In particular, since the castings themselves can no longer meet the stringent requirement for precision and the hitherto used grinding has not delivered the coveted results, we are concentrating on the use of milling as a final operation in producing turbine blades from Inconel 738LC for aerospace industry. The goal is to find such milling parameters that would be not only efficient in respect to the machining time, but would also lead to a high quality surface necessary for components' reliability and a long service life. In order to do the quality inspection, the milled surface is described by several surface integrity parameters obtainable by non-destructive X-ray diffraction technique. This approach is based on assumption [1] that structure and microstructure of the surface layer, residual stresses,

microstrains and dislocation density directly affect the durability, and hence, the service life of components that are under dynamic loads.

The very use of nickel super-alloys in aerospace industry is based on their favourable properties stemming from complicated microstructure and the real structure of individual crystalline phases that is distinguished by a complex character of grain boundaries, presence of defects such as vacancies, dislocations, stacking faults and residual stresses. Moreover, from this point of view the grinding is not a very considerate processing of the material since it in can trigger off local melting resulting in presence of usually undesirable white layer and cracks [2]. On the other hand, the enormous evolution in the material of tools for milling has facilitated substantial reduction in costs due to increase of cutting speed, e.g. up to ten times faster machining with whisker reinforced corundum [3] when compared with traditional cermet WC-Co tool tips. The use of ceramic materials in tool tips represents another bonanza to the milling process as their high melting temperature limits the thermally activated tool wear and favours the less harsh abrasive mechanism.

In this study, we present an investigation of *macroscopic residual stresses, microstrains, grain sizes and phase composition* of milled turbine blades with special attention to the effect of *tool feed, tool wear and the cutter orientation or work-piece angle*.

## 2. Samples under investigation

The analysed bodies were casted from Inconel 738LC super-alloy and subsequently machined by 3 axis milling. The choice of milling parameters was done according to Design-Of-Experiments (DOE) method in such a manner that will enable to ascertain their effect on the selected surface integrity parameters. The machining conditions, which are briefly summarized in Table 1, were set according to DOE to compare (i) tool wear while keeping the other machining parameters constant. Furthermore, we are able to assess from the diffraction measurements (ii) the influence of cutter orientation and work-piece angle and (iii) the effect of tool feed. As the castings were not exactly the same from the geometrical point of view, they were coarse milled in order to ensure the constant cutting depth during the final milling. The very reproducibility of both the diffraction measurements and the milling process was verified on three blades that were machined under exactly the same conditions. The assessment of the (ii) parameter was possible because three areas corresponding to three different places with the cutter orientation and the work-piece angle as seen in Fig. 1.

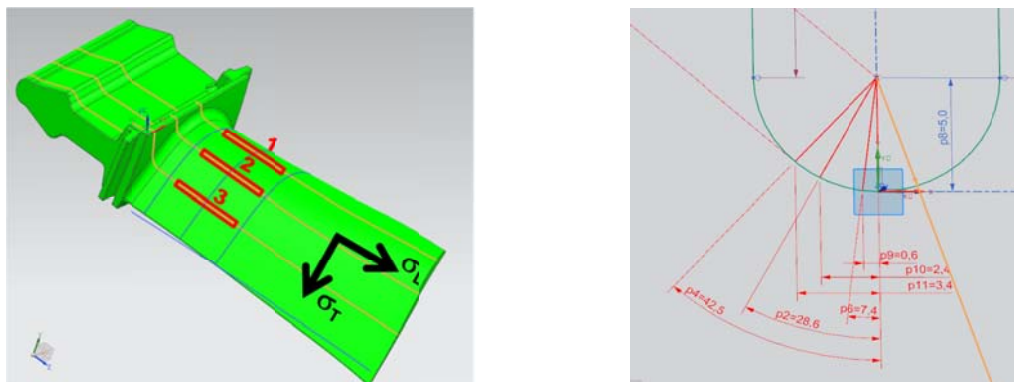


Figure 1. Scheme of the measured surface on samples with marked directions of stress determination  $\sigma_L$ ,  $\sigma_T$  and the measured areas 1, 2 and 3 (left) and corresponding average values of the tool tilt in respect to the work-piece (right).

Table 1. Working and cutting conditions used in the experiments.

Sample	1	3	4	5	6	7	8	9	10	11	14
Tool diameter [mm]	10/R5										
Character of tool feed	parallel milling with pushed tool										
Cooling	flooding by cooling liquid										
Axial depth $a_p$ [mm]	2 x 0.5										
Number of teeth [-]	4										
Cutting feed [mm]	534	534	696	567	534	534	534	643	534	378	626
Cutting speed [m/min]	42	42	42	37	42	42	42	42	42	37	49
Tool's run	1 <sup>st</sup>	1 <sup>st</sup>	2 <sup>nd</sup>	1 <sup>st</sup>	2 <sup>nd</sup>	1 <sup>st</sup>	1 <sup>st</sup>	2 <sup>nd</sup>	3 <sup>rd</sup>	1 <sup>st</sup>	1 <sup>st</sup>

### 3. Experimental techniques

The measurements were performed on a  $\theta/\theta$  goniometer X'Pert PRO MPD. Positioning of the blade to the desired areas was done by in-house system with 6 degree of freedom, namely x,y,z translation, rotation and two tilts; with control of the surface position having  $5\mu\text{m}$  accuracy employing laser triangulation system [4].  $\text{MnK}\alpha$  radiation was used for diffraction measurements aiming at residual stresses calculations,  $\text{CrK}\alpha$  radiation for microstrains and grain size computation and  $\text{CoK}\alpha$  radiation for phase composition determination. Unfortunately, it is not within the powers of X-ray diffraction to distinguish between the two in nickel super-alloys most commonly occurring phases of  $\gamma$  and  $\gamma'$ . Both crystalize in f.c.c. with  $\gamma$  having the austenitic structure and  $\gamma'$  being the main precipitation phase, moreover, their lattice parameters  $a_\gamma$ ,  $a_{\gamma'}$  are very similar [5] with the lattice mismatch  $\delta = 2(a_\gamma - a_{\gamma'})/(a_\gamma + a_{\gamma'})$  in the order of 0.x % resulting in almost perfect overlapping of diffraction profiles.

The diffraction line  $\{311\}$  of  $\gamma$  and  $\gamma'$  phases was measured in order to obtain macroscopic residual stresses. Values of macroscopic residual stresses  $\sigma_L$  and  $\sigma_T$ , see Fig. 1, were calculated from lattice deformations determined from  $2\theta^{311}(\sin^2\psi)$  plots following Winholtz-Cohen algorithm [6] and using the X-ray elastic constants  $\frac{1}{2}s_2 = 6.57 \cdot 10^{-6} \text{ MPa}^{-1}$ ,  $s_1 = -1.56 \cdot 10 \cdot 10^{-6} \text{ MPa}^{-1}$  computed according to Eshelby-Kröner approach [7]. Diffraction angle  $2\theta^{311}$  was taken as a centre of gravity of the  $\{311\}$  diffraction doublet  $\text{MnK}\alpha$ .

Single-line Voigt function method [8] was applied for calculations of microstrains and average grain sizes using  $\{111\}$  diffraction line of  $\gamma$  and  $\gamma'$  phases. Both parameters were determined from all three areas 1, 2, 3 oriented in two directions given by stresses  $\sigma_L$  and  $\sigma_T$ .

### 4. Results

The values of macroscopic residual stresses in both measured directions are summarized in Tab. 2 in such a manner that would enable to consider the effect of tool wear. Microstrains  $e$  and grain sizes  $D$  averaged over all values in areas 1, 2, 3 and both directions are in Tab. 3. The impact of tool feed can be seen from Tab. 4 where residual stresses obtained in the direction of tool feed  $\sigma_T$  and perpendicularly to it  $\sigma_L$  are shown for all three investigated areas. Eventually the example of phase analysis is in Fig. 2.

Table 2. Surface macroscopic residual stresses  $\sigma_L$  and  $\sigma_T$ , MPa; analysis of tool wear effect.

Sample	1, 3, 7 and 8		6		10	
Tool's run	new – 1 <sup>st</sup>		used – 2 <sup>nd</sup> run		used – 3 <sup>rd</sup> run	
Area	$\langle\sigma_L\rangle$	$\langle\sigma_T\rangle$	$\sigma_L$	$\sigma_T$	$\sigma_L$	$\sigma_T$
1	$7 \pm 23$	$-298 \pm 20$	$-225 \pm 29$	$-455 \pm 16$	$-104 \pm 14$	$-492 \pm 21$
2	$187 \pm 19$	$-195 \pm 22$	$141 \pm 35$	$-194 \pm 35$	$44 \pm 35$	$-379 \pm 47$
3	$159 \pm 26$	$-189 \pm 22$	$214 \pm 24$	$2 \pm 32$	$226 \pm 25$	$-271 \pm 23$

Table 3. Microstrains  $e$  and grain sizes  $D$  averaged over all values in areas 1, 2, 3 and both directions.

	Area 1	Area 2	Area 3	direction $L$	direction $T$
$\langle D \rangle$ , nm	39	48	50	48	43
$\langle e \rangle$ , $10^{-4}$	61	61	57	62	58

Table 4. Surface macroscopic residual stresses  $\sigma_T$  and  $\sigma_L$ , MPa; analysis of the tool feed effect.

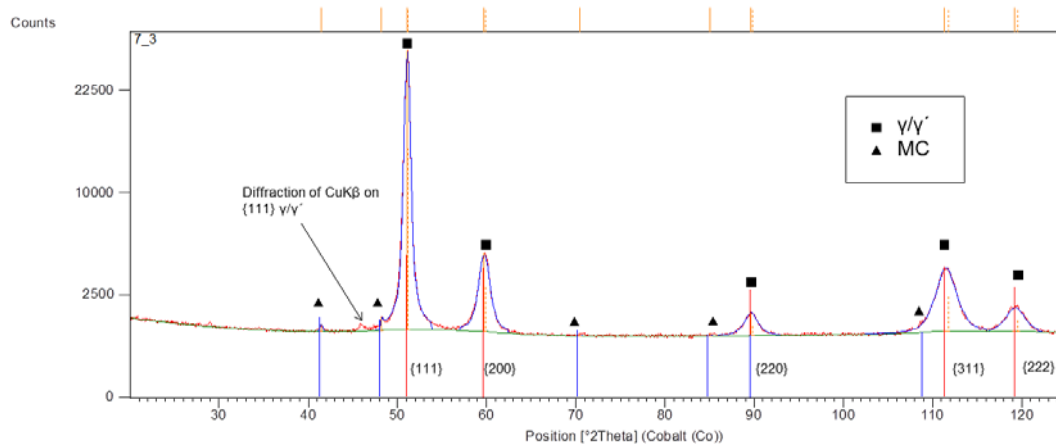
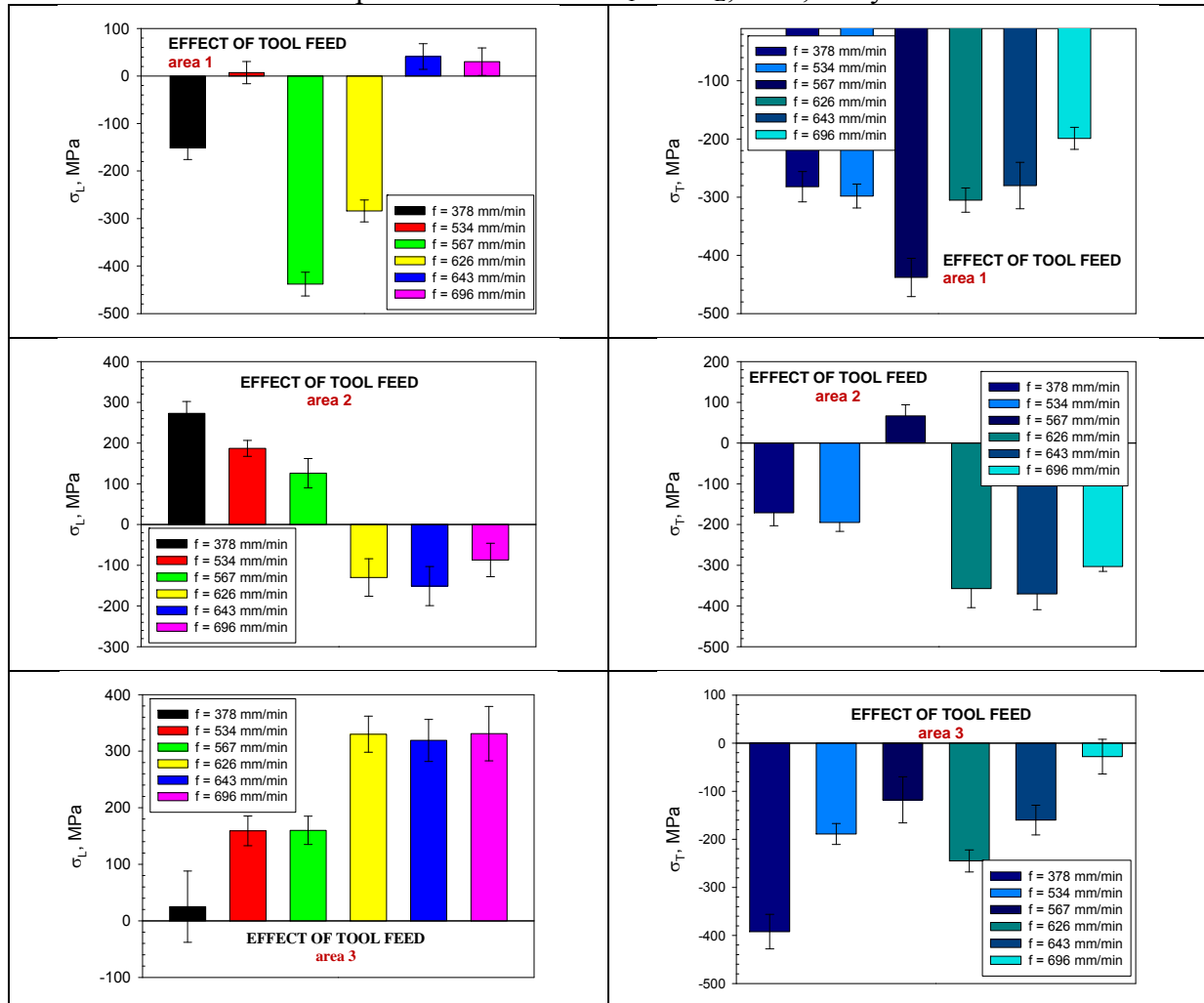


Figure 2. Phase analysis of selected diffraction pattern from area 3 on blade 7. Phase ID revealed presence of  $\gamma$ ,  $\gamma'$  and a univalent Metal Carbide (MC) phase.

## 6. Discussion

Nickel super-alloys belong to difficult-to-machine materials and are generally prone to mechanical hardening during machining. Mechanical hardening is causing significantly heterogeneous behaviour with manifestations of unstable chip formation or vibrations. Ultimately, the quality of the machined surface is poor which is reflected in shorter service life. Analyses of several surface integrity parameters are only one important step in the process of finding the right machining parameters. Once this is combined with cutting forces measurements and economic feasibility check, a solid ground for new manufacturing process is laid. Here, we present such analyses of initial research stage aiming at 3 axis milling; the other stages will include 4 and 5 axis milling.

X-ray diffraction can significantly contribute to this process by non-destructive assessment of relevant parameters of surface quality. First of all, it offers comparatively fast check of the presence of unwanted phases such as tetragonal  $\sigma$  phase as seen in Fig. 2. Secondly, it is capable of giving information about residual stresses that can be directly related to the surface quality. The results in the chapter above amply illustrate this.

Microstrains and grain sizes are seldom studied in the case of nickel super-alloys machining, even though microstrain strongly correlates with microhardness [9]. Although debatable and problematic, the average values of microstrains and grain sizes reflect the essence of the individual results which is that no significant differences in both measured directions were observed and that area *I* had distinctly lower values of grain sizes.

## 7. Conclusions

- There is no indication in any diffraction pattern of amorphous material presence in the surface layer and only crystalline phases of  $\gamma$  and  $\gamma'$  and a univalent Metal Carbide (MC) phase were found. Neither the  $M_6C$  or  $M_{23}C_6$  or the detrimental tetragonal  $\sigma$  phase were present in the surface. Therefore, it has been verified that no precipitation of undesirable phases on the surface after the milling with selected parameters was observed.
- The average grain size (Tab. 3) is the smallest in area *I* and it rises with increasing tool tilt, i. e. in the areas 2 and 3. This effect of crystallite crushing is caused by the squeezing of the material by the tool that has the smallest tilt in the area *I* of  $7^\circ$ , see Fig. 1 (right), the effective diameter of the tool is here only 1.3 mm with effective cutting speed of 5 m/min. Area *I* is also distinguished by higher cutting temperature.
- Neither monotonous rise nor monotonous decline of  $D$  and  $e$  was observed with increasing tool feed, but systematically lower values were recorded when feed reached 534 mm/min. Machining with new tool always led to lower values of  $D$  and  $e$  when compared with the worn tool which is caused by more effective cutter edge.
- Macroscopic residual stresses  $\sigma_T$  are in the absolute majority of measured areas, with only two exceptions, compressive. Yet, the stresses in the direction perpendicular to the tool feed, i.e.  $\sigma_L$ , are mostly tensile. The notable exceptions are the  $\sigma_L$  in area *I* which are always compressive which is most probably the effect of chip squeezing resulting in much larger tool wear and changes in torque and power values of milling process.
- Tool wear has appreciable effect on the values of residual stresses in both analysed directions. Most likely due to the cutting edge blunting, the values are moving to the tensile stresses, i.e. growing. Only the area 3 in the  $L$  direction has different character, where the stresses are decreasing towards more pronounced compression. In this area, the

cutter tilt is the largest exceeding  $42^\circ$  as seen in Fig. 2 (right) and the mesh is of another kind especially in respect to the geometry of chip formation and overall energetic balance.

- Values of residual stress are sensitive to the tool feed in all three areas 1, 2 and 3, but do not follow monotonous dependence.
- The area 3 appears to be problematic, since only unfavourable tensile residual stresses are observed in the  $L$  direction, see Tab. 4. This issue can be eliminated in the following stage of 4 axis milling. Stresses in the  $T$  direction are with only one exception always compressive, we therefore suggest to avoid the  $f = 567$  mm/min.
- The residual stresses  $\sigma_L$  have quite oscillatory character on the tool feed value in the area 1, the surface roughness in this area was beyond the limits of tolerance.
- Considering the area 2, values of tool feed exceeding 600 m/min seem to be the most appropriate since they result only in compressive residual stresses.

*Based on the performed analyses, the following recommendation can be made. For the upcoming stage of 4 axis milling it would be most convenient to use tool feed exceeding 600 m/min and have a similar cutter orientation and work-piece angle as in the area 2.*

### **Acknowledgements**

This research was carried out in the frame of research projects TA02011031 of Technology Agency of the Czech Republic.

### **References**

- [1] A. G. Youtsos, Residual stress and its effect on fracture and fatigue, Springer 2006.
- [2] M.C. Shaw, Surface Melting in Grinding Operations?, Ann. CIRP 33 (1984) 221-223.
- [3] I.A. Choudhury, M.A. El-Baradie, Machinability of nickel-base super alloys: a general review, J. Mat. Proc. Technol. 77 (1998) 278-284.
- [4] Z. Pala, N. Ganev, J. Drahokoupil, Surface layers study of bulky samples by X'Pert PRO diffractometer, Materials Structure 15 (2008) k46-k47.
- [5] J. Li, R.P. Wahi, Investigation of  $\gamma/\gamma'$  lattice mismatch in the polycrystalline nickel –base superalloy IN738LC: Influence of heat treatment and creep deformation, Acta metall. mater. 43 (1995) 507-517.
- [6] R.A. Winholtz, J.B. Cohen, Generalized Least-Squares Determination of Triaxial Stress States by X-ray Diffraction and the Associated Errors, Aust. J. Phys. 41 (1988), 189-199.
- [7] E. Kröner, Allgemeine Kontinuumstheorie der Versetzungen und Eigenspannungen, Archive for Rational Mechanics and Analysis 4, (1959/60) 273-334.
- [8] Th.H.de Keijser, J.I. Langford, E.J. Mittemeijer, A.B.P.Vogels, Use of the Voigt function in a single-line method for the analysis of X-ray diffraction line broadening, J. Appl. Crystallogr. 15 (1989) 308–314.
- [8] M. Čerňanský, N. Ganev, J. Barcal, J. Drahokoupil, K. Kolařík, Diffraction analysis of iron materials after surface machining, Zeitschrift fur Kristallographie 2 (2006) pp 369-374.